Published in final edited form as:
Mol Cancer Ther. 2015 November ; 14(11): 2665–2673. doi:10.1158/1535-7163.MCT-15-0394.

A novel fully-humanised 3D skin equivalent to model early melanoma invasion

David S Hill[1], **Neil D P Robinson**[2], **Matthew P Caley**[3], **Mei Chen**[4], **Edel A O'Toole**[3], **Jane L Armstrong**[1,5], **Stefan Przyborski**[2,*], and **Penny E Lovat**[1,*]

[1]Dermatological Sciences, Institute of Cellular Medicine, Newcastle University, Newcastle-upon-Tyne, UK

[2]School of Biological and Biomedical Sciences, Durham University, Durham, UK

[3]Centre for Cutaneous Research, Barts and the London SMD, Queen Mary University of London, Blizard Institute, London, UK

[4]Norris Comprehensive Cancer Centre, University of Southern California, Los Angeles, CA, USA

[5]Faculty of Applied Sciences, University of Sunderland, Sunderland, UK

Abstract

Metastatic melanoma remains incurable, emphasising the acute need for improved research models to investigate the underlying biological mechanisms mediating tumour invasion and metastasis, and to develop more effective targeted therapies to improve clinical outcome. Available animal models of melanoma do not accurately reflect *human* disease and current *in vitro* human skin equivalent models incorporating melanoma cells are not fully representative of the human skin microenvironment.

We have developed a robust and reproducible, fully-humanised 3D skin equivalent comprising a stratified, terminally differentiated epidermis and a dermal compartment consisting of fibroblast-generated extracellular matrix. Melanoma cells incorporated into the epidermis were able to invade through the basement membrane and into the dermis, mirroring early tumour invasion *in vivo*.

Comparison of our novel 3D melanoma skin equivalent with melanoma *in situ* and metastatic melanoma indicates this model accurately recreates features of disease pathology, making it a physiologically representative model of early radial and vertical growth phase melanoma invasion.

Keywords

melanoma; humanised 3D skin equivalent; early tumour invasion

[*]Corresponding author concerning skin and melanoma cell biology: Dr Penny Lovat Dermatological Sciences, Institute of Cellular Medicine The Medical School Newcastle University Framlington Place, Newcastle upon Tyne, NE2 4HH United Kingdom penny.lovat@ncl.ac.uk Tel: +44 191 2227170 . [*]Corresponding author concerning 3D in vitro skin technology: Professor Stefan Przyborski School of Biological and Biomedical Sciences Durham University, South Road, Durham DH1 3LE United Kingdom stefan.przyborski@durham.ac.uk Tel: +44 191 3343988 .

There are no financial conflicts of interest.

Europe PMC Funders Author Manuscripts

Introduction

Cutaneous metastatic melanoma remains one of the most deadly forms of cancer, with a rapidly increasing incidence, mortality and public health burden. Although early stage melanoma is largely curable through surgical resection, continued 5-year survival rates of only 5-19% for advanced disease (1) reflect the lack of consistently beneficial treatments for metastatic melanoma. Improved research models are therefore urgently needed to investigate the underlying biological mechanisms mediating tumour invasion and subsequent metastasis, and to facilitate the development of more effective targeted therapies to improve clinical outcome.

Human skin comprises an upper epidermal layer containing mainly keratinocytes in close association with melanocytes, and a lower dermal layer containing multiple cell types including fibroblasts that synthesise extracellular matrix (ECM) components to support cellular growth (2). Keratinocytes form a proliferative basal layer and differentiate as they move towards the surface of the skin, while melanocytes, the precursor cells of melanoma, proliferate less frequently and remain at the epidermal-dermal junction where they interact with basal layer keratinocytes to regulate tanning of the skin in response to UV radiation (3). A basement membrane, composed of matrix molecules including laminin isoforms and type IV, VII and XVII collagens separate melanocytes and keratinocytes from the papillary dermis (4). However, when melanocytes become transformed, hyper-proliferative and migratory melanoma cells invade through the basement membrane into the dermis. Therefore models that aim to investigate early melanoma development must recreate the microenvironment of this distinct cellular niche (5).

While mouse xenograft models of melanoma in immunocompromised mice are commonly used to investigate tumour development, progression and therapeutic response they do not accurately recreate the microenvironment of human melanoma at either the primary or distant site. As such, these models cannot recapitulate the initial events leading to early invasion through the basement membrane or dissemination of melanoma cells throughout the skin and to subsequent metastatic sites. Furthermore, while spontaneous mouse melanoma models (6-8) are useful for investigating the early stages of *mouse* melanoma development, significant differences between the architecture of human and rodent skin (9), as well as differences observed in the histopathological features of human and murine melanoma subtypes (10) make it difficult to extrapolate results from these studies into a clinically relevant context.

To more accurately investigate early stage *human* melanoma, full-thickness *in vitro* skin equivalent models incorporating melanoma cells have been developed, which allow investigation of melanoma migration and invasion from the epidermis into the dermis (11-14). However, such equivalents comprise a dermal component created from fibroblasts embedded in bovine or rat-tail collagen, which as well as contracting over time leading to distortion and disruption of the equivalent, are not representative of the normal human skin microenvironment as they include non-human ECM components. Alternatively, while de-cellularised human skin models offer a human skin microenvironment, variability between

donors results in inconsistent melanoma migration, which impacts the reproducibility of these assays (15).

The present study describes a novel *in vitro* model for the investigation of early melanoma invasion, such as that which occurs in radial and vertical growth phase melanoma, within a fully-humanised cutaneous microenvironment. We have developed a unique full-thickness three dimensional (3D) skin equivalent (organotypic skin culture) through the incorporation of an inert porous scaffold (16) with appropriate pore sizes to support the 3D growth and cell-cell contact of primary human dermal fibroblasts. Fibroblasts are stimulated to produce their own ECM constituents (17, 18), forming a stable dermal component that is physiologically representative of normal human skin. Following addition of primary human keratinocytes, crosstalk between fibroblasts and keratinocytes facilitates the development of a permissive microenvironment conducive to long-term culture (19). This is consistent with previous studies showing the stratum corneum of skin equivalents formed on fibroblast-derived matrix contains a considerably higher concentration of natural moisturising factor compared to animal collagen based skin equivalents, thus allowing cultures to be maintained for up to 20 weeks (20).

Seeding melanoma cells *onto* the dermal equivalent prior to the incorporation of primary human keratinocytes, rather than implanting melanoma spheroids directly into the dermis (21), or suspending melanoma cells in hydrogel (22), places the melanoma cells in their original micro-environmental niche within the skin, resulting in subsequent proliferation and nest formation at the epidermal-dermal junction prior to invasion through the basement membrane. We demonstrate that active invasion of melanoma cells results in breakdown of basement membrane components type IV and VII collagens, accurately recapitulating the pattern of early melanoma invasion observed in human cutaneous tumours *in vivo,* thus providing a valuable tool to investigate mechanisms mediating melanoma initiation and early stages of disease progression.

Materials and Methods

Cell culture

Primary human neonatal foreskin fibroblasts (CellnTec; Stauffcherstr, Switzerland) were cultured in Media A (Table 1) for up to 7 passages. Immortalised mouse embryonic 3T3 fibroblasts (ATCC-CCL-92) were cultured in Media D. Following informed consent, primary human keratinocytes derived from surplus skin obtained from patients (aged between 20 and 55) undergoing routine surgery (for which full ethical approval was obtained; National Research Ethics reference, Newcastle and North Tyneside 1 08/H0906195 for all studies with human tissue) were isolated by incubating the skin in dispase (Scientific Laboratory Supplies, Nottingham, UK) for 12-18 h at 4^{o}C to separate the epidermis from the dermis before dissociating the epidermis with trypsin/EDTA (Scientific Laboratory Supplies) (23) for 5 min at 37^{o}C and subsequently cultured in Media E for up to 2 passages. Keratinocytes were then further co-cultured with mitomycin C (Sigma-Aldrich, Poole, UK) treated 3T3 feeder cells (24) at 1:1 ratio in Media B (based on (25)) for up to 3 passages, changing the media every day. Following detachment with trypsin/EDTA, keratinocytes were subsequently incubated with an equal volume of soybean trypsin

inhibitor (Sigma-Aldrich) and centrifuged at 300 g for 5 min prior to re-suspension in fresh culture media and subsequent culture. Human metastatic melanoma cell line, SK-mel-28 (LGC Standards; ATCC-HTB-72,) and the primary human melanoma cell line, WM35 (Coriell Cell Repositories, Philadelphia) were obtained in 2011, and are tested every 6 months for Melan-A expression by immunofluorescence, with *BRAF* mutational status confirmed by real time polymerase chain reaction (26), and cultured in Media A as previously described (27). All cells were cultured at 37ºC in a humidified atmosphere with 5% CO_2 in air.

Human skin equivalent preparation

12-well format Alvetex® scaffold (Reinnervate Ltd, Reprocell group) were pre-treated with 70% ethanol in a 6-well plate according to the manufacturer's instructions. 2.0×10^6 primary human neonatal foreskin fibroblasts were seeded onto Alvetex® in 100 μl Media A and incubated at 37°C, in a humidified atmosphere of 5% CO_2 in air for 1.5 hours. 9 ml of Media A + 100 μg/ml ascorbic acid (Sigma-Aldrich) were subsequently applied to the bottom of each well to gently flood the insert prior to incubation for a further 18 days, changing media every 3.5 days, to allow the formation of a dermal equivalent. Dermal equivalents were subsequently washed with 10 ml phosphate buffered saline (PBS; Sigma-Aldrich) prior to the addition of 4 ml Media B to the outer side of the insert such that the bottom of each dermal equivalent was in contact with the media. To establish a melanoma 3D equivalent, 2.0×10^4 melanoma cells were applied to the dermal equivalent in 100 μl Media B and incubation at 37°C continued for a further 3 hours. In the meantime, primary human keratinocytes were harvested by differential trypsinisation, discarding the 3T3 feeder cells, and 2.0×10^6 keratinocytes seeded onto dermal equivalents (with or without melanoma cells) in 100 μl Media B and incubation continued for a further 3 hours. 5ml of Media B was then applied to the outer side of each well to gently flood the inside of the insert prior to further incubation at 37°C for 3 days, changing the media every day. On day 21, the insert was removed from the 6-well plate and placed into a well insert holder in a deep petri dish (Reinnervate Ltd, Reprocell group) on the middle rung of the stand. 30 ml of Media C was then added to the dish such that the bottom of the equivalent was in contact with the media but the upper surface remained exposed to the air and incubation continued at 37°C in 5% CO_2 for 14 days, changing the media every 3.5 days, to allow the formation of a full-thickness skin equivalent.

Scanning electronmicroscopy (SEM)

Skin equivalent or primary tissue samples of normal human skin were fixed in a 1:1 mix of DMEM media and double strength fixation buffer (16% PFA (Sigma-Aldrich), 25% glutaraldehyde (Agar Scientific, Stansted, UK), 0.2 M sodium cacodylate (Agar Scientific)) for 5-10 mins at room temperature. Samples were then transferred to a new tube and incubated in single strength fixation buffer (8% PFA, 12.5% glutaraldehyde, 0.1 M sodium cacodylate) at 4°C for 1 hour prior to washing in PBS three time for 5 minutes each. Samples were subsequently cut into 2-3 mm^2 squares and immersed in post-fixation buffer (1% osmium tetroxide (Agar Scientific)) in 0.1M sodium cacodylate) at 4°C for 60 minutes before washin in 0.1M sodium cacodylate buffer twice for 10 minutes each. Following dehydration though a series of ethanol washes (30%, 50%, 70%, 80%, 90%, 95% and 100%)

Europe PMC Funders Author Manuscripts

each for 15 minutes, samples were then dried using a critical point dryer (Baltec CPD030, Pfäffikon ZH, Switzerland), coated in 5 nm of platinum using a Cressington Coating System 328 (Cressington Scientific Instruments, Watford, UK) and visualised using a Leica S5200 scanning electron microscope (Leica Microsystems, Milton Keynes, UK).

Immunofluorescent analysis of skin biomarkers

Formalin-fixed, paraffin-embedded primary human tissue samples derived from an *in situ* melanoma or an AJCC stage IV metastatic melanoma were used as a comparative to 3D human melanoma skin equivalents. All samples were processed for haematoxylin and eosin staining or immunohistochemistry as previously described (28, 29). 5 μM sections were incubated with 1:1000 mouse anti-human type III collagen (kindly supplied by Dr Rachel Watson, Manchester University) (Abcam, Cambridge, UK; ab23445), 1:1000 mouse anti-type IV collagen (Abcam; ab6586), 1:400 rabbit anti-type VII collagen (kindly supplied by Dr Mei Chen (30)), 1:1000 rabbit anti-cytokeratin 1 (Abcam; ab93652), 1:1000 mouse anti-cytokeratin 14 (Abcam; ab7800), 1:1000 mouse anti-involucrin (Abcam; ab68), or 1:250 mouse anti-Melan-A (Abcam; ab731) primary antibodies diluted in PBS + 5% BSA overnight at 4°C. Primary antibody binding was detected with secondary Alexa Fluor 488 goat anti-mouse (Life Technologies, Paisley, UK) or Alexa Fluor 488 goat anti-rabbit antibodies (Life Technologies) and cell nuclei counter stained with DAPI (1 μg/ml; Life Technologies) diluted in PBS + 5% BSA for 1 hour at room temperature. Sections were finally mounted under glass coverslips in Vectorshield mounting media (Vector Laboratories, Peterborough, UK) and visualised using either a Leica DMI3000B (Leica Microsystems) or an Axioimager Z2 (Carl Zeiss Ltd, Cambridge, UK).

Results

Generation of a full-thickness human skin equivalent

Alvetex® porous polymer scaffolds were used to create a full-thickness human skin equivalent in the absence of any animal matrix components (Figure 1). Pre-treatment of Alvetex® by immersion in 70% ethanol rendered it hydrophilic allowing media and cells to enter the 3D matrix. Alvetex® scaffolds were subsequently washed with culture media to remove the ethanol and seeded with primary human neonatal foreskin fibroblasts, prior to culture for 18 days in Media A (Table 1) supplemented with ascorbic acid to promote synthesis of collagen polypeptides through the processing of pro-collagens to collagen α-chains (17). Primary human keratinocytes isolated from the epidermis of normal human skin were then seeded onto the upper surface and cultured for 3 days in Media B. The upper surface was subsequently exposed at the air/liquid interface for 14 days to induce keratinocyte differentiation, while the lower surface remained in contact with Media C, resulting in the formation of a full-thickness human skin equivalent.

Cell numbers, media components and time intervals for each step of the protocol were optimised to allow full scaffold colonisation by dermal fibroblasts (Figure 2a) and the establishment of an intact, fully stratified epidermis with key morphological features of a stratum basale, stratum spinosum and stratum corneum (Figure 2b, 20x magnification; Figure 2c, 10x magnification). Electron micrographs indicate the structure and porosity of

the Alvetex® scaffold membrane (Figure 2d) supporting fibroblast growth in three dimensions and facilitating the establishment of a full-thickness human skin equivalent (Figure 2e) with clear morphological similarities to normal human skin (Figure 2f).

Primary human keratinocytes and fibroblasts in organotypic culture form a humanised skin microenvironment

Normal human skin comprises a dermal layer and a multi-layered epidermis, each layer of which displays a distinct protein expression profile (Figure 3a). The dermis contains extracellular matrix components, including type I and III collagen, while the epidermis is characterised by the expression of various cytokeratins that are differentially regulated within different layers of the epidermis, reflecting the progressive stages of normal human keratinocyte differentiation. Histological analysis of our established 3D skin equivalent (Figure 3b) demonstrated morphological similarities to that of normal human skin (Figure 3c), and a comparative commercially available model (Mattek EpidermFT; Figure 3d); in particular the presence of a fully developed stratum corneum was evident indicating keratinocyte differentiation and barrier formation.

Immunofluorescent staining also revealed the expression of human type III, IV and VII collagen, cytokeratin 1 and 14 as well as involucrin (Figure 3), to varying degrees in the 3D skin equivalent, normal human skin and the Mattek EpidermFT. Dermal fibroblasts contained within the 3D skin equivalent for 35 days clearly expressed type III collagen (Figure 3t), which albeit not as abundant as expression observed in normal human skin (Figure 3u) nevertheless indicated the production of human extrcellular matrix, critical to the long-term maintenance of the skin equivalent. In contrast however, less human type III collagen expression was observed in the Mattek EpidermFT (Figure 3v), likely due to their construction mainly being based on the use of bovine type I collagen that may suppresses further ECM production by the dermal fibroblasts. The 3D skin equivalent model also demonstrated production of human type I collagen (data not shown).

The basement membrane components type IV and VII collagens were clearly expressed at the epidermal-dermal junction of both the 3D skin equivalent (Figure 3n,q) and normal human skin (Figure 3o,r), indicating interaction between fibroblasts and keratinocytes and synthesis of a *de novo* basement membrane. However, while expression of type IV collagen was partially observed between the epidermal and dermal layers within the Mattek EpidermFT model, there was no evidence for the organised expression of type VII collagen (Figure 3p,s). It is possible however, that the Mattek EpidermFT model may not have been cultured for sufficient time to enable type VII collagen organisation and the formation of a basement membrane comparable to normal skin (31).

Expression of cytokeratin 14 by keratinocytes within the 3D skin equivalent also indicated the formation of a stratum basale (Figure 3k), resembling that of normal human skin (Figure 3l). Keratinocytes within the 3D skin equivalent appeared to undergo normal differentiation as demonstrated by the expression of cytokeratin 1 and involucrin in suprabasal and terminal layer keratinocytes, indicative of stratum spinosum and stratum granulosum formation respectively (Figure 3h,e), and again indicative of the pattern of epidermal differentiation observed in normal human skin (Figure 3i,f). Furthermore, while expression of cytokeratin

14 (Figure 3m) was observed in Mattek EpidermFT, cytokeratin I (Figure 3j) and involucrin (Figure 3g) expression was less well defined, indicating formation of a stratum basale but ineffective keratinocyte differentiation in this model. The establishment of an organotypic skin equivalent on Alvetex® scaffolds therefore accurately recreates the microenvironment of normal human skin. This was subsequently used to investigate melanoma cell behaviour *in vitro*.

Melanoma cell invasion through the basement membrane of fully humanised 3D skin equivalents recreates the progressive histopathological features of melanoma invasion in human skin

The potential for human melanoma cell lines derived from either primary or metastatic tumours to invade the pore structure of Alvetex® scaffolds was verified in the absence of primary fibroblasts (data not shown). To model melanoma invasion, metastatic melanoma cells were applied to pre-established fibroblast-containing Alvetex® dermal equivalents prior to the incorporation of keratinocytes at a slightly lower ratio (100:1) to the physiological ratio of keratinocytes to melanocytes in normal human skin (36:1) (32), in order to prevent tumour cell over growth within the epidermis prior to the observation of dermal invasion. Histological staining of a 3D skin equivalent 2 weeks post-incorporation with metastatic SK-mel-28 melanoma cells demonstrated the development of melanoma nests at the epidermal/dermal junction (Figure 4a), verified by the expression of the melanocyte lineage-specific marker Melan-A (Figure 4e). Immunofluorescent staining for the human basement membrane components type IV collagen (Figure 4i) and type VII collagen (Figure 5a) 2 weeks after the incorporation of melanoma cells into the skin equivalent revealed intact expression of both markers and clear localisation of melanoma cells above both type IV (Figure 4m,q) and type VII collagen (Figure 5e,i). However, culture for a further 2 weeks resulted in the invasion of Melan-A-positive melanoma cells into the dermal component (Figure 4b,f), accompanied by disruption of type IV collagen (Figure 4j) and loss of type VII collagen (Figure 5b). Furthermore, co-staining for Melan-A and either type IV collagen (Figure 4n,r) or type VII collagen (Figure 5f,j) demonstrated disruption of these basement membrane components coincided with melanoma invasion, indicating SK-mel-28 melanoma cells actively invade from the epidermis into the dermis of the skin equivalent through the basement membrane. Similar results were also obtained with skin equivalents incorporating Melan-A-positive primary WM35 melanoma cells, where again tumour invasion through the basement membrane, albeit less than metastatic SK-mel-28, was observed with a concurrent disruption of type IV collagen at 4 weeks (Supplementary Figure 1).

To validate whether invasion of melanoma cells within a 3D skin equivalent accurately reflects the progressive stages of clinical disease, the effect of melanoma cells on type IV and VII collagen were investigated in a formalin-fixed paraffin embedded *in situ* melanoma or in a primary tumour derived from a patient with metastatic disease. Histological staining and Melan-A immunostaining of the melanoma *in situ* (Figure 4c,g) confirmed a minimally invasive tumour accompanied by continuous and intact expression of both type IV (Figure 4k) and type VII collagen (Figure 5c) at the epidermal/dermal junction. Co-immunostaining demonstrated that in pre-invasive melanomas, cells are located above type IV (Figure 4o,s) and type VII collagen (Figure 5g,k) indicating an intact basement membrane, which reflects

the histopathological features observed in 3D skin equivalents after 2 weeks post-incorporation with melanoma cells. Conversely, histology and immunostaining for the expression of Melan-A in the metastatic melanoma (Figure 4d,h) revealed highly invasive tumour cells with disrupted type IV (Figure 4l) and VII collagen (Figure 5d) expression. Active invasion of this advanced metastatic melanoma, resulting in loss or disruption of type IV collagen (Figure 4p,t) and type VII collagen (Figure 5h,l), similarly reflected the histopathological features observed in 3D skin equivalents 4 weeks after incorporation of SK-mel-28 metastatic melanoma cells. Collectively, these data indicate our novel 3D skin equivalent accurately recreates the progressive histopathological features of melanoma invasion in human skin and the applicability of this novel organotypic skin model as a valuable tool for the investigation of early melanoma invasion.

Discussion

The present study demonstrates the generation of a novel full-thickness human skin equivalent bearing morphological and structural similarity to normal human skin within 35 days. We have optimised and validated a protocol for the construction of an organotypic skin model from primary human fibroblasts and keratinocytes that accurately recreates the microenvironment of normal human skin, as demonstrated by the production of human extracellular matrix component type III collagen, as well as the distinct expression profile of basement membrane proteins type IV and VII collagen, and epidermal differentiation markers cytokeratin 14, and involucrin. Incorporation of melanoma cells into their original environmental niche at the epidermal/dermal junction demonstrates tumour cells retain their proliferative and invasive potential, forming melanoma clusters before invading though the basement membrane into the dermis.

Comparative histopathological features observed in primary melanomas derived from differing American Joint Committee on Cancer (AJCC) disease stages (33), confirm the 3D skin equivalent model is physiologically representative of clinical disease. Conversely, while Mattek EpidermFT expressed type IV collagen, the lack of human type III and VII collagen expression suggests the reduced longevity of this model will limit its use for the investigation of less invasive melanoma cells.

Interestingly, our data demonstrate that while invasion of both SK-mel-28 and WM35 melanoma cells through the basement membrane of the 3D skin equivalent resulted in the breakdown and disruption of type IV collagen there appeared to be an increase in type IV collagen surrounding invading tumour cells, consistent with previous observations showing increased type IV collagen expression parallels melanoma progression (34, 35) and which is directly required for melanoma metastasis (36). However, increased type IV collagen in this context is likely independent of its function as a basement membrane component as it does not form a continuous membrane structure. Collectively these data support the validity of the 3D skin equivalent as a representative model of early melanoma invasion *in vivo*. Furthermore, since chemokines and growth factors including IGF-1 (37) are known to drive melanoma invasion, the present model may also offer a means through which to study the effect of modulating such factors within melanoma cells on early tumour invasion.

In addition to confirming the presence of distinct skin layers within the skin equivalent, our data demonstrate the presence of regular compacted areas within the epidermis (Figure 2b), which may represent important microenvironmental niche areas of the skin where skin stem cells may reside (38-41). Importantly these data confer the additional potential utility of our 3D skin equivalent model for the investigation of dermal stem cell and hair follicle biology.

Furthermore, while the model presented is an allogeneic skin equivalent specifically developed for the investigation of melanoma invasion, it may be readily adapted into an autologous setting for the investigation of immunological pathologies, or adapted through the addition of endothelial cells to the lower surface for studies of angiogenesis within the skin or development of tumour neovasculature. Grafting the 3D skin equivalent onto immunocompromised mice, in line with studies in alternative skin equivalent models (42), may also represent a useful means through which to investigate tumour cell dissemination from the skin to secondary sites.

In summary, the 3D skin equivalent model presented represents a robust and reproducible assay that is widely applicable to dermatological research, mimicking the morphology and microenvironment of normal human skin more accurately than previous assays. The demonstration of the applicability of this model for the investigation of the early stages of human melanoma invasion therefore renders it a valuable tool for defining and evaluating urgently required novel drug targets and personalised therapies.

Supplementary Material

Refer to Web version on PubMed Central for supplementary material.

Acknowledgments

Financial Information

This work was predominantly supported in the UK by grants from The JGW Patterson Foundation (D.S. Hill, J. L. Armstrong, P. E. Lovat) and The Newcastle Healthcare Charity (P. E. Lovat) with additional support from the National Council for Reduction, Refinement and Replacement of Animals in Research (NC3Rs; D.S. Hill, P. E. Lovat), the Biotechnology and Biological Sciences Research Council (BBSRC; N. D. P. Robinson and S. Przyborski) and DEBRA UK (M. P. Caley, E. A. O'Toole). Work in The United States of America was supported by The National Institute of Health (M. Chen, grants RO1 AR47981 and RO1 AR33625).

References

1. Sandru A, Voinea S, Panaitescu E, Blidaru A. Survival rates of patients with metastatic malignant melanoma. Journal of medicine and life. 2014; 7:572–6. [PubMed: 25713625]
2. Simpson CL, Patel DM, Green KJ. Deconstructing the skin: cytoarchitectural determinants of epidermal morphogenesis. Nat Rev Mol Cell Biol. 2011; 12:565–80. [PubMed: 21860392]
3. Bandarchi B, Jabbari CA, Vedadi A, Navab R. Molecular biology of normal melanocytes and melanoma cells. Journal of clinical pathology. 2013; 66:644–8. [PubMed: 23526597]
4. Fleischmajer R, Utani A, MacDonald ED, Perlish JS, Pan TC, Chu ML, et al. Initiation of skin basement membrane formation at the epidermo-dermal interface involves assembly of laminins through binding to cell membrane receptors. J Cell Sci. 1998; 111(Pt 14):1929–40. [PubMed: 9645941]
5. Boyce ST. Design principles for composition and performance of cultured skin substitutes. Burns : journal of the International Society for Burn Injuries. 2001; 27:523–33. [PubMed: 11451611]

6. Dhomen N, Reis-Filho JS, da Rocha Dias S, Hayward R, Savage K, Delmas V, et al. Oncogenic Braf induces melanocyte senescence and melanoma in mice. Cancer Cell. 2009; 15:294–303. [PubMed: 19345328]
7. Kumasaka MY, Yajima I, Hossain K, Iida M, Tsuzuki T, Ohno T, et al. A novel mouse model for de novo Melanoma. Cancer Res. 2010; 70:24–9. [PubMed: 20048069]
8. Dankort D, Curley DP, Cartlidge RA, Nelson B, Karnezis AN, Damsky WEJ, et al. Braf(V600E) cooperates with Pten loss to induce metastatic melanoma. Nat Genet. 2009; 41:544–52. [PubMed: 19282848]
9. Khavari PA. Modelling cancer in human skin tissue. Nat Rev Cancer. 2006; 6:270–80. [PubMed: 16541145]
10. Walker GJ, Soyer HP, Terzian T, Box NF. Modelling melanoma in mice. Pigment Cell Melanoma Res. 2011; 24:1158–76. [PubMed: 21985222]
11. Li L, Fukunaga-Kalabis M, Herlyn M. The Three-Dimensional Human Skin Reconstruct Model: a Tool to Study Normal Skin and Melanoma Progression. Journal of Visualized Experiments. 2011
12. Monteiro-Riviere NA, Inman AO, Snider TH, Blank JA, Hobson DW. Comparison of an in vitro skin model to normal human skin for dermatological research. Microscopy research and technique. 1997; 37:172–9. [PubMed: 9144629]
13. Berking C, Herlyn M. Human skin reconstruct models: a new application for studies of melanocyte and melanoma biology. Histol Histopathol. 2001; 16:669–74. [PubMed: 11332722]
14. Meier F, Nesbit M, Hsu MY, Martin B, Van Belle P, Elder DE, et al. Human melanoma progression in skin reconstructs : biological significance of bFGF. Am J Pathol. 2000; 156:193–200. [PubMed: 10623667]
15. Eves P, Layton C, Hedley S, Dawson RA, Wagner M, Morandini R, et al. Characterization of an in vitro model of human melanoma invasion based on reconstructed human skin. Br J Dermatol. 2000; 142:210–22. [PubMed: 10730751]
16. Bokhari M, Carnachan RJ, Cameron NR, Przyborski SA. Novel cell culture device enabling three-dimensional cell growth and improved cell function. Biochem Biophys Res Commun. 2007; 354:1095–100. [PubMed: 17276400]
17. Peterkofsky B. The effect of ascorbic acid on collagen polypeptide synthesis and proline hydroxylation during the growth of cultured fibroblasts. Archives of biochemistry and biophysics. 1972; 152:318–28. [PubMed: 4342111]
18. Nusgens BV, Humbert P, Rougier A, Colige AC, Haftek M, Lambert CA, et al. Topically applied vitamin C enhances the mRNA level of collagens I and III, their processing enzymes and tissue inhibitor of matrix metalloproteinase 1 in the human dermis. J Invest Dermatol. 2001; 116:853–9. [PubMed: 11407971]
19. Boehnke K, Mirancea N, Pavesio A, Fusenig NE, Boukamp P, Stark HJ. Effects of fibroblasts and microenvironment on epidermal regeneration and tissue function in long-term skin equivalents. Eur J Cell Biol. 2007; 86:731–46. [PubMed: 17292509]
20. El Ghalbzouri A, Commandeur S, Rietveld MH, Mulder AA, Willemze R. Replacement of animal-derived collagen matrix by human fibroblast-derived dermal matrix for human skin equivalent products. Biomaterials. 2009; 30:71–8. [PubMed: 18838164]
21. Vorsmann H, Groeber F, Walles H, Busch S, Beissert S, Walczak H, et al. Development of a human three-dimensional organotypic skin-melanoma spheroid model for in vitro drug testing. Cell Death Dis. 2013; 4:e719. [PubMed: 23846221]
22. Leight JL, Tokuda EY, Jones CE, Lin AJ, Anseth KS. Multifunctional bioscaffolds for 3D culture of melanoma cells reveal increased MMP activity and migration with BRAF kinase inhibition. Proc Natl Acad Sci U S A. 2015; 112:5366–71. [PubMed: 25870264]
23. Sharpe GR, Gillespie JI, Greenwell JR. An increase in intracellular free calcium is an early event during differentiation of cultured human keratinocytes. FEBS Lett. 1989; 254:25–8. [PubMed: 2776884]
24. Vollmers A, Wallace L, Fullard N, Hoher T, Alexander MD, Reichelt J. Twoand three-dimensional culture of keratinocyte stem and precursor cells derived from primary murine epidermal cultures. Stem cell reviews. 2012; 8:402–13. [PubMed: 21892602]

25. Stark HJ, Baur M, Breitkreutz D, Mirancea N, Fusenig NE. Organotypic keratinocyte cocultures in defined medium with regular epidermal morphogenesis and differentiation. J Invest Dermatol. 1999; 112:681–91. [PubMed: 10233757]
26. Hiscutt EL, Hill DS, Martin S, Kerr R, Harbottle A, Birch-Machin M, et al. Targeting X-linked inhibitor of apoptosis protein to increase the efficacy of endoplasmic reticulum stress-induced apoptosis for melanoma therapy. J Invest Dermatol. 2010; 130:2250–8. [PubMed: 20520630]
27. Armstrong JL, Hill DS, McKee CS, Hernandez-Tiedra S, Lorente M, Lopez-Valero I, et al. Exploiting Cannabinoid-Induced Cytotoxic Autophagy to Drive Melanoma Cell Death. J Invest Dermatol. 2015
28. Knight E, Murray B, Carnachan R, Przyborski S. Alvetex(R): polystyrene scaffold technology for routine three dimensional cell culture. Methods in molecular biology (Clifton, NJ). 2011; 695:323–40. [PubMed: 21042981]
29. Ellis RA, Horswell S, Ness T, Lumsdon J, Tooze SA, Kirkham N, et al. Prognostic impact of p62 expression in cutaneous malignant melanoma. J Invest Dermatol. 2014; 134:1476–8. [PubMed: 24270664]
30. Chen M, Petersen MJ, Li HL, Cai XY, O'Toole EA, Woodley DT. Ultraviolet A irradiation upregulates type VII collagen expression in human dermal fibroblasts. J Invest Dermatol. 1997; 108:125–8. [PubMed: 9008222]
31. Betz P, Nerlich A, Wilske J, Tubel J, Wiest I, Penning R, et al. The time-dependent rearrangement of the epithelial basement membrane in human skin wounds--immunohistochemical localization of collagen IV and VII. International journal of legal medicine. 1992; 105:93–7. [PubMed: 1520644]
32. Hoath SB, Leahy DG. The organization of human epidermis: functional epidermal units and phi proportionality. J Invest Dermatol. 2003; 121:1440–6. [PubMed: 14675195]
33. Balch CM, Gershenwald JE, Soong SJ, Thompson JF, Atkins MB, Byrd DR, et al. Final version of 2009 AJCC melanoma staging and classification. J Clin Oncol. 2009; 27:6199–206. [PubMed: 19917835]
34. Rotte A, Martinka M, Li G. MMP2 expression is a prognostic marker for primary melanoma patients. Cellular oncology (Dordrecht). 2012; 35:207–16. [PubMed: 22669775]
35. Hofmann UB, Westphal JR, Waas ET, Zendman AJ, Cornelissen IM, Ruiter DJ, et al. Matrix metalloproteinases in human melanoma cell lines and xenografts: increased expression of activated matrix metalloproteinase-2 (MMP-2) correlates with melanoma progression. Br J Cancer. 1999; 81:774–82. [PubMed: 10555745]
36. Shaverdashvili K, Wong P, Ma J, Zhang K, Osman I, Bedogni B. MT1-MMP modulates melanoma cell dissemination and metastasis through activation of MMP2 and RAC1. Pigment Cell Melanoma Res. 2014; 27:287–96. [PubMed: 24387669]
37. Friedl P, Wolf K. Tumour-cell invasion and migration: diversity and escape mechanisms. Nat Rev Cancer. 2003; 3:362–74. [PubMed: 12724734]
38. Ghazizadeh S, Taichman LB. Organization of stem cells and their progeny in human epidermis. J Invest Dermatol. 2005; 124:367–72. [PubMed: 15675956]
39. Wong VW, Levi B, Rajadas J, Longaker MT, Gurtner GC. Stem cell niches for skin regeneration. International journal of biomaterials. 2012; 2012:926059. [PubMed: 22701121]
40. Bickenbach JR. Identification and behavior of label-retaining cells in oral mucosa and skin. Journal of dental research. 1981; 60(Spec No C):1611–20. [PubMed: 6943171]
41. Taylor G, Lehrer MS, Jensen PJ, Sun TT, Lavker RM. Involvement of follicular stem cells in forming not only the follicle but also the epidermis. Cell. 2000; 102:451–61. [PubMed: 10966107]
42. Kiowski G, Biedermann T, Widmer DS, Civenni G, Burger C, Dummer R, et al. Engineering melanoma progression in a humanized environment in vivo. J Invest Dermatol. 2012; 132:144–53. [PubMed: 21881586]

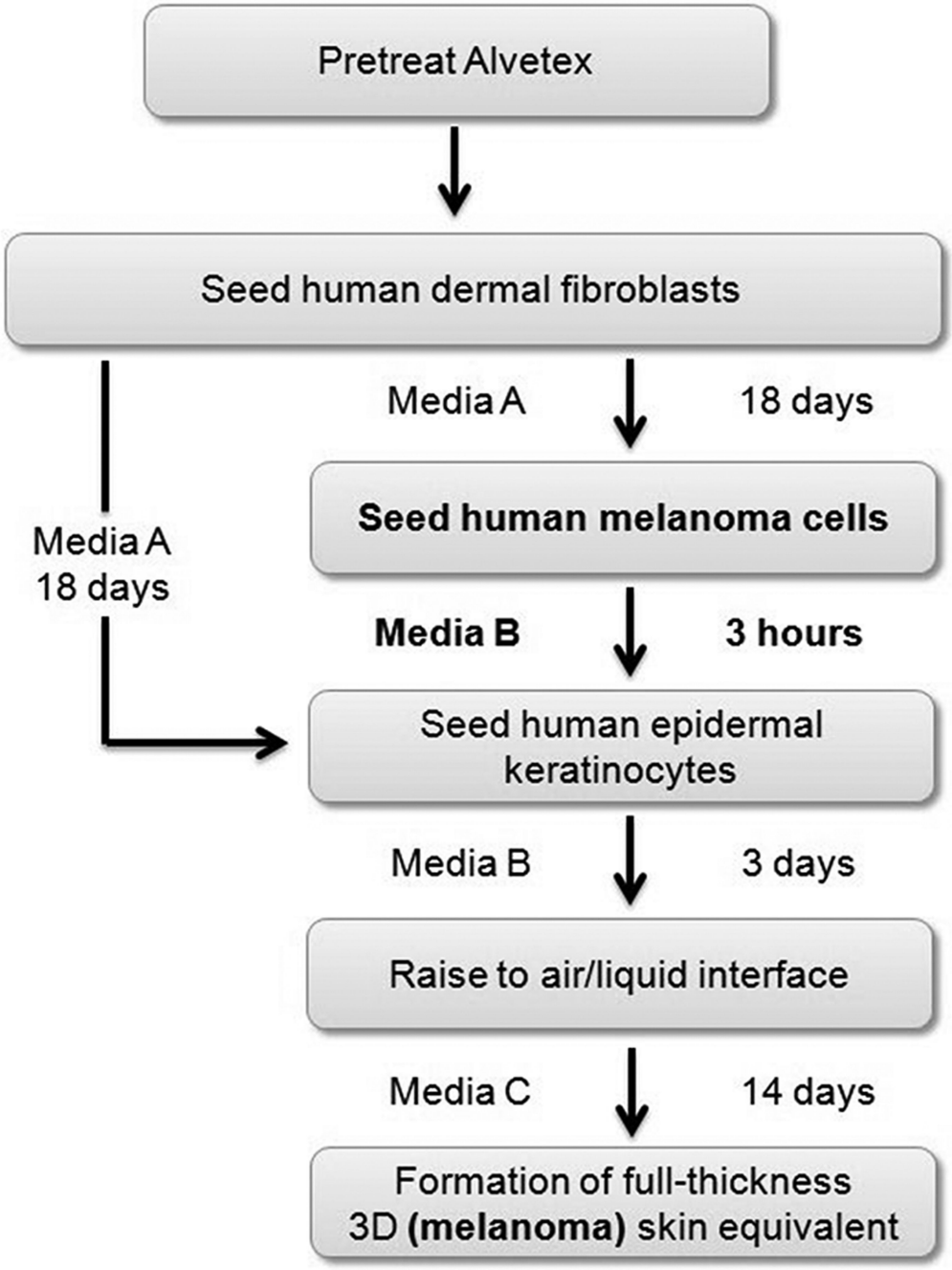

Figure 1. Schematic protocol for the formation of full-thickness human skin equivalents

Pretreat inert Alvetex® polymer scaffold in 70% ethanol before thoroughly washing in Media A, then seed with 5.0×10^5 human dermal fibroblasts. Culture fibroblast-seeded Alvetex® in Media A for 18 days to create a dermal equivalent. If establishing a melanoma full thickness skin equivalent, seed 2.0×10^4 metastatic melanoma cells onto the dermal equivalent and culture in Media B for 3 hours prior to the addition of primary human keratinocytes. Alternatively, to create a full thickness skin equivalent, add 2.0×10^6 keratinocytes directly onto the dermal equivalent. Culture the (melanoma) equivalent fully

submerged in Media B for 3 days before exposing the upper surface of the equivalent to the air–liquid interphase and continuing culture for 14 days with the lower surface in contact with Media C (See methods for full protocol).

Europe PMC Funders Author Manuscripts

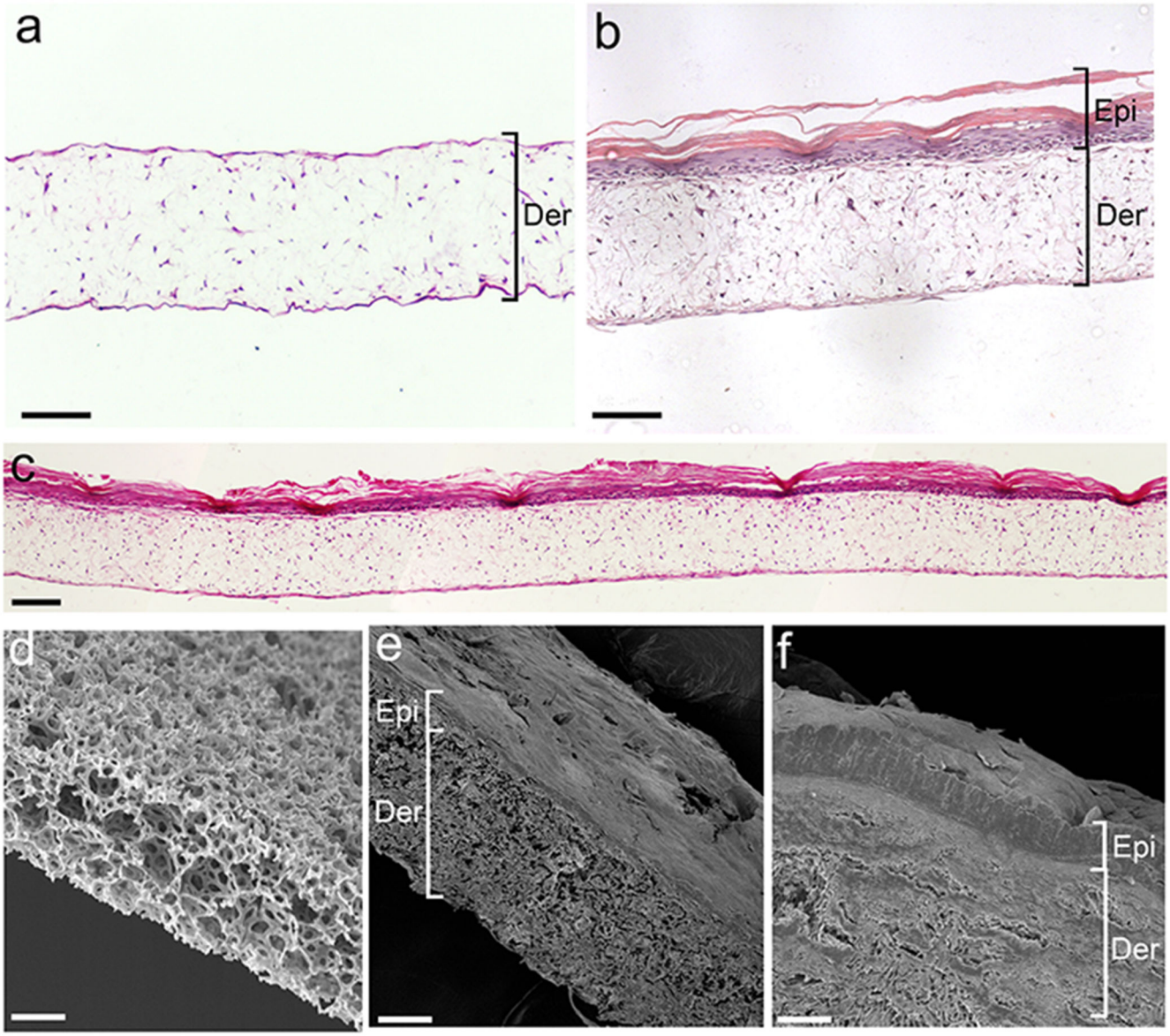

Figure 2. Validation of dermal and epidermal structure in full-thickness human skin equivalents

a) Representative photomicrographs of haematoxylin and eosin (H&E) stained Alvetex® seeded with human dermal fibroblasts after culture in Media A for 18 days. b&c) Representative photomicrographs showing H&E stained 35 day full-thickness human skin equivalents at 20x and 10x magnification respectively. d) Representative electronmicrographs of a non-cellularised Alvetex® scaffold, e) 35 day full-thickness human skin equivalent or f) normal human skin. a-c scale bars, 100 μm; d-f scale bars, 75 μm; Epi, epidermis; Der, dermis.

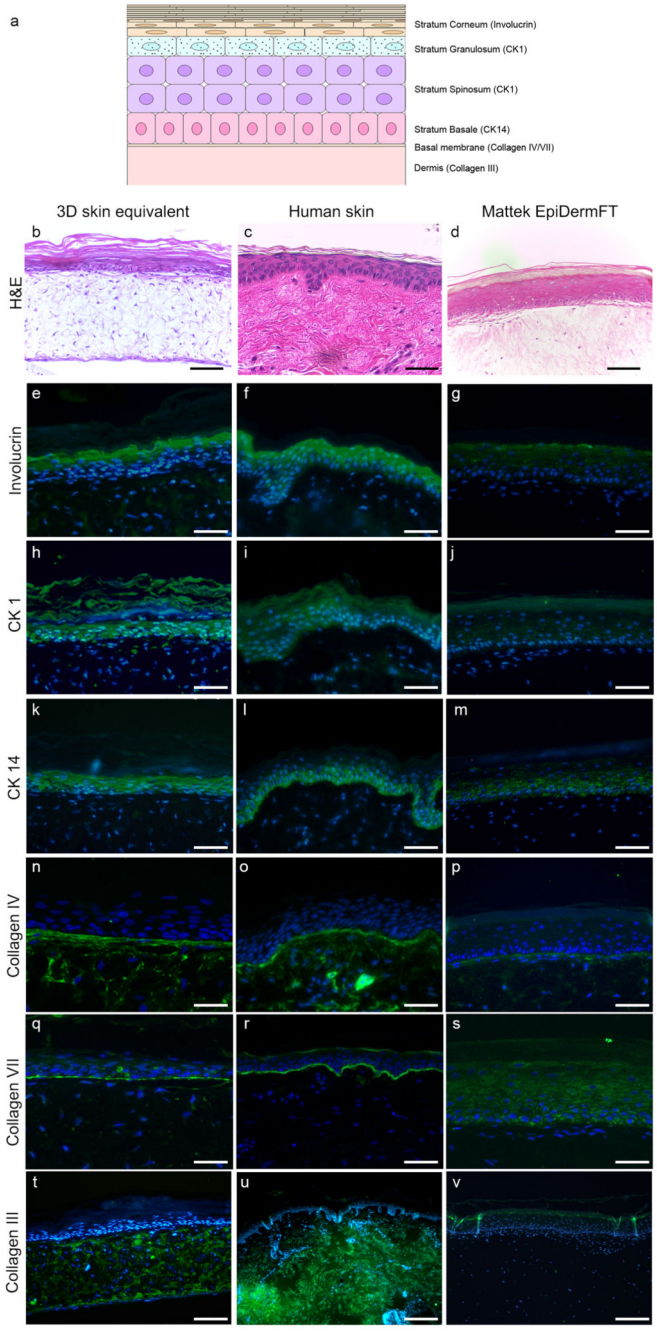

Figure 3. Expression of epidermal, dermal or basement membrane markers in full-thickness human skin equivalents compared to human skin and Mattek EpiDermFT

a) Schematic illustrating dermal and epidermal protein marker expression. b-d) Representative photomicrographs showing an H&E stained full-thickness human skin equivalent (b), normal human skin (c) or a Mattek EpiDermFT (d). e) Representative fluorescent photomicrographs for the expression of involucrin (e-g), cytokeratin I (CK 1, h-j), cytokeratin XIV (CK 14, k-m), type IV collagen (n-p), type VII collagen (q-r) or type III collagen (t-v) in full-thickness human skin equivalents, normal human skin or Mattek EpiDermFT. b-d & t-v scale bars, 75 μm; e-s scale bars, 25 μm.

Europe PMC Funders Author Manuscripts

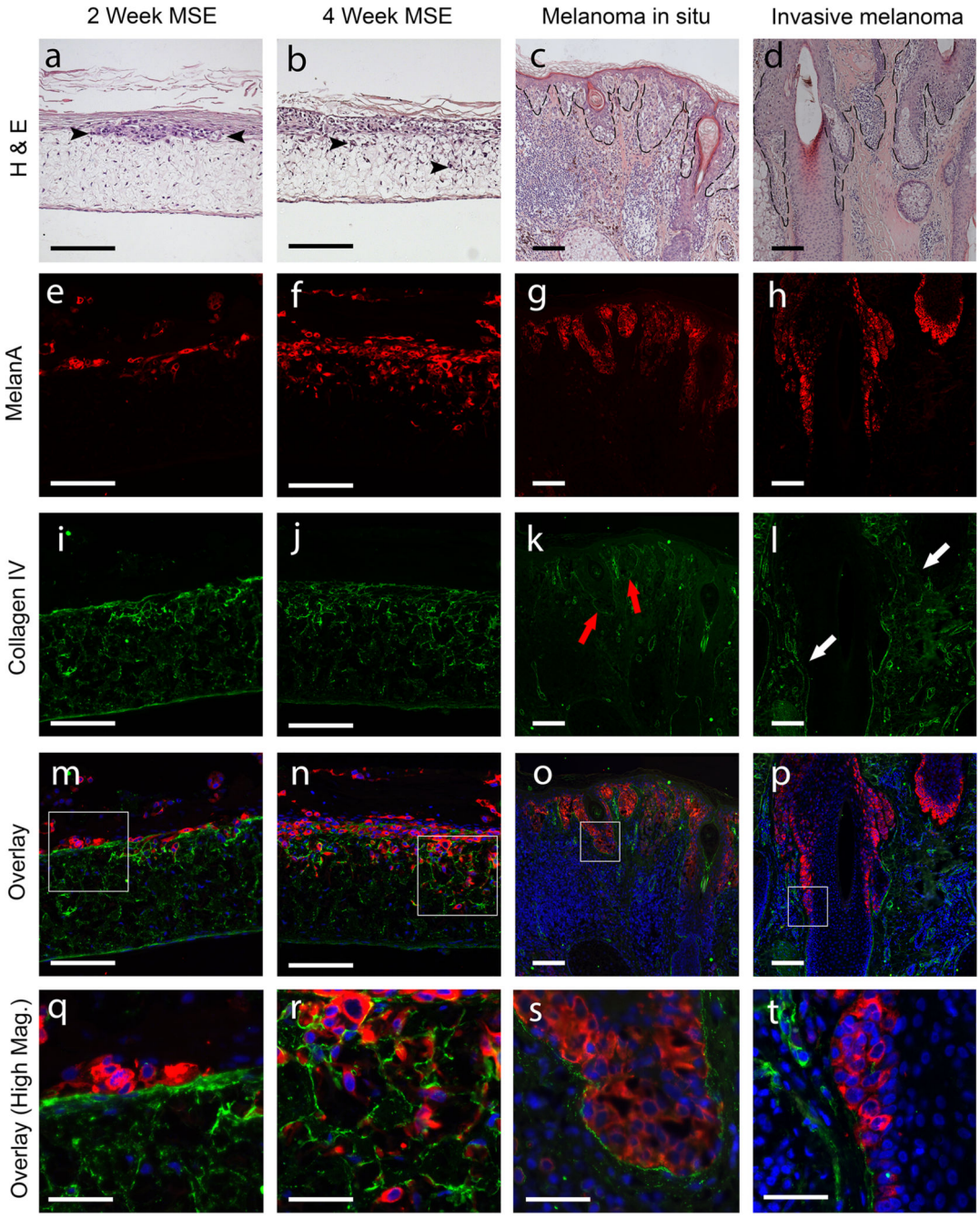

Figure 4. Early cutaneous melanoma invasion in full-thickness human skin equivalents results in disruption of basement membrane component type IV collagen

Representative photomicrographs showing H&E stained full thickness melanoma skin equivalents (MSE) at 2 weeks (a) or 4 weeks (b) post-inoculation with melanoma cells, highlighting clusters/nests of melanoma cells at the dermal/epidermal junction at week 2, which subsequently invade through the basement membrane at week 4 (black arrow heads); and H&E stained sections of a melanoma *in situ* (c) or a primary superficial spreading malignant melanoma (d; invasive melanoma) (black dotted lines illustrate the tumour boundary). Representative fluorescent photomicrographs for the expression of Melan-A

(red; e-h) or type IV collagen (green; i-l) in 2 week (e and i) or 4 week (f and j) MSEs, melanoma *in situ* (g and k), or an invasive melanoma (h and l) (Red arrows illustrate intact type IV collagen while white arrows illustrate where type IV collagen is lost). m-p) Overlay fluorescent photomicrographs showing relative expression of Melan-A and type IV collagen in 2 week (m) and 4 week (n) MSEs, melanoma *in situ* (o), and an invasive melanoma (p; note melanoma cells have invaded from right to left) with white boxes highlighting area magnified in panels q-t (blue = DAPI). q-t) 63x magnification of Melan-A and type IV collagen in 2 week (q) and 4 week (r) MSEs, melanoma *in situ* (s), and an invasive melanoma (t). a-p scale bars, 100 μm; q-t scale bars, 25 μm.

Europe PMC Funders Author Manuscripts

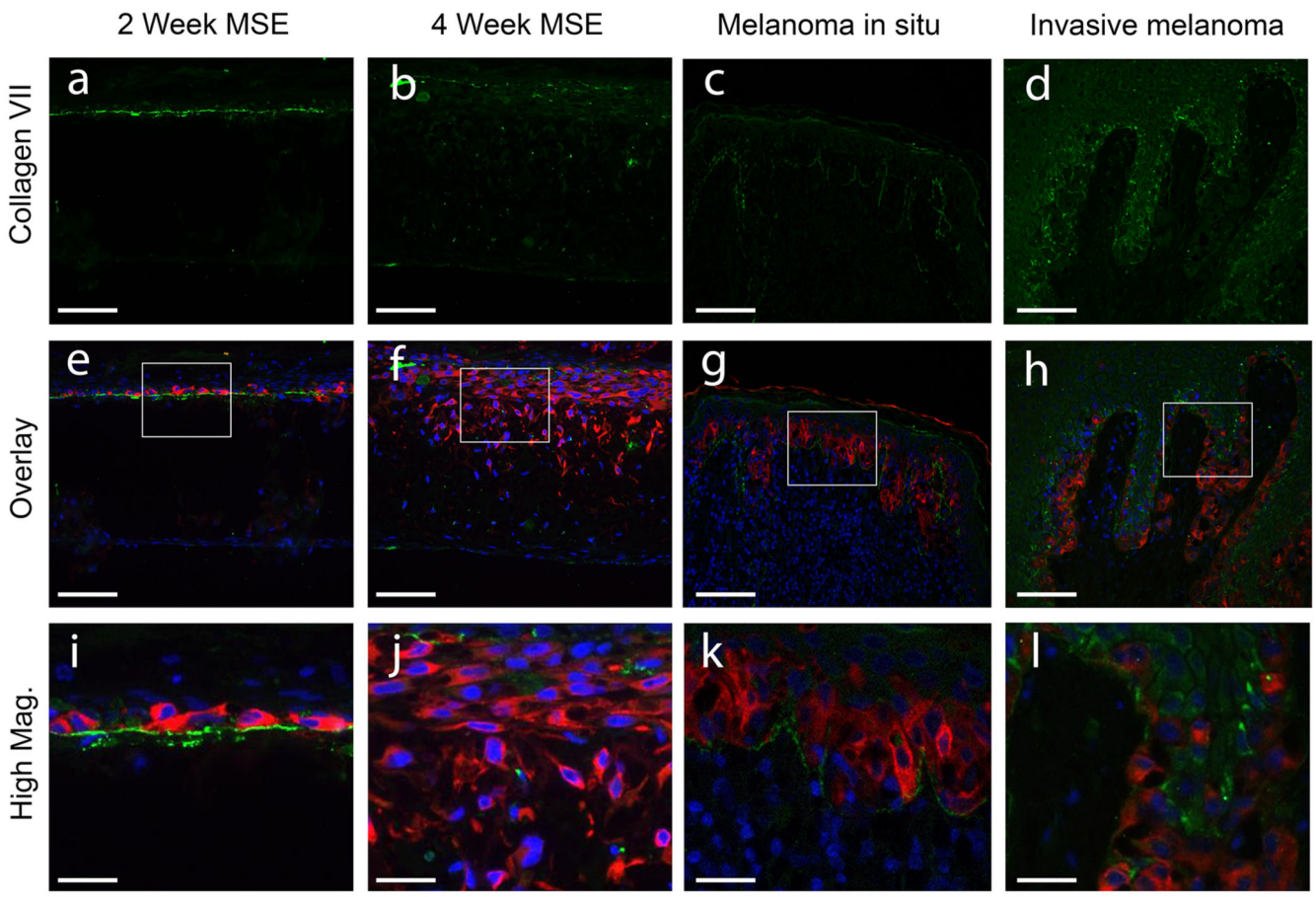

Figure 5. Early cutaneous melanoma invasion in full-thickness human skin equivalent results in disruption of basement membrane component type VII collagen

a-d) Representative fluorescence photomicrographs of type VII collagen (green) expression in 2 week (a) and 4 week (b) melanoma skin equivalents (MSE), melanoma *in situ* (c), and a primary superficial spreading malignant melanoma (d; invasive melanoma). e-h) Overlay fluorescence photomicrographs showing relative expression of Melan-A (red) and type VII collagen in 2 week (e) and 4 week (f) MSEs, melanoma *in situ* (g) and an invasive melanoma (h) with white boxes highlighting area magnified in panels i-l (blue = DAPI). i-l) 63x magnification of Melan-A and type VII collagen in 2 week (i) and 4 week (j) MSEs, melanoma *in situ* (k), and an invasive melanoma (l). a-h scale bars, 100 μm; i-l scale bars, 25 μm.

Europe PMC Funders Author Manuscripts

Table 1

Media components for the production of full-thickness melanoma skin equivalents

Volume or weight and final concentration of each component in Media A-E required for producing full-thickness melanoma skin equivalents (see methods section for use of each media).

Media	Component (stock conc.)	Volume or Weight	Final Concentration
A	Dulbecco's Modified Eagles Medium	500 ml	-
	Fetal Calf Serum	50 ml	≈10%
	Penicillin/Streptomycin/Amphotericin	5 ml	≈1%
B	Dulbecco's Modified Eagles Medium	375 ml	-
	Ham's F12 Nutrient Mixture	125 ml	-
	Chelex-treated Fetal Calf Serum	25 ml	≈5%
	Cholera toxin (0.85 mg/ml)	5 µl	8.5 ng/ml
	Hydrocortisone (0.5 mg/ml)	400 µl	0.4 µg/ml
	Insulin (10 mg/ml)	250 µl	5 µg/ml
	Adenine (6 mg/ml)	2 ml	24 µg/ml
	Recombinant Human Epidermal Growth Factor (0.2 mg/ml)	50 µl	10 ng/ml
	Penicillin/Streptomycin/Amphotericin	5 ml	≈1%
C	Dulbecco's Modified Eagles Medium.	375 ml	-
	Ham's F12 Nutrient Mixture	125 ml	-
	Fetal Calf Serum	50 ml	≈10%
	Cholera toxin (0.85 mg/ml)	5 µl	8.5 ng/ml
	Hydrocortisone (0.5 mg/ml)	400 µl	0.4 µg/ml
	Recombinant Human Epidermal Growth Factor (0.2 mg/ml)	50 µl	10 ng/ml
	Transferin (10 mg/ml)	250 µl	5 µg/ml
	Penicillin/Streptomycin/Amphotericin	5 ml	≈1%
	L-Ascorbic acid (10 mg/ml) added fresh	100 µl per 10 ml media	100 µg/ml
D	Dulbecco's Modified Eagles Medium	500 ml	-
	Iron-fortified Newborn Calf Serum	25 ml	≈5%
	Penicillin/Streptomycin/Amphotericin	5 ml	≈1%
E	MCDB153 with L-Glutamine, 28 mM HEPES	500 ml	-
	Histidine	18.65 mg	240 µM
	Isoleucine	49.2 mg	750 µM
	Methioninen	6.7 mg	90 µM
	Phenylalanine	7.45 mg	90 µM

Media	Component (stock conc.)	Volume or Weight	Final Concentration
	Tryptophan[■]	4.6 mg	45 μM
	Tyrosine[■]	9.775 mg	100 μM
	Ethanolamine (98% w/v)[■]	3.05 μl	100 μM
	Phosphorylethanolamine[■]	7.05 mg	100 μM
	Calcium chloride (1M)[■]	20 μl	40 μM
	Sodium bicarbonate	588 mg	15 mM
	Human Keratinocyte Growth Supplement[●]	5 ml	≈1%
	Penicillin/Streptomycin/Amphotericin[◆]	5 ml	≈1%
	Adjust to pH 7.2		

The suppliers of each component are indicated by superscript.

◆Scientific Laboratory Supplies Ltd, Nottingham UK;

■Sigma-Aldrich Company Ltd, Dorset, UK;

●Life Technologies Ltd, Paisley, UK;

○Bio-Rad Laboratories Ltd, Hemel Hempstead, UK.

Europe PMC Funders Author Manuscripts